Effect of tropical cyclones on the Stratosphere-Troposphere Exchange observed using satellite observations over north Indian Ocean

M. Venkat Ratnam[1*], S. Ravindra Babu[2], Siddarth Shankar Das[3], Ghouse Basha[1], B.V. Krishnamurthy[4] and B.Venkateswararao[2]

[1]National Atmospheric Research Laboratory (NARL), Gadanki, India.
[2]Jawaharlal Nehru Technological University, Hyderabad, India.
[3]Space Physics Laboratory (SPL), VSSC, Trivandrum, India.
[4]CEBROSS, Chennai, India.

*vratnam@narl.gov.in , 08585-272123 (phone), 08585-272018 (Fax)

Abstract

Tropical cyclones play an important role in modifying the tropopause structure and dynamics as well as stratosphere-troposphere exchange (STE) processes in the Upper Troposphere and Lower Stratosphere (UTLS) region. In the present study, the impact of cyclones that occurred over the North Indian Ocean during 2007-2013 on the STE processes is quantified using satellite observations. Tropopause characteristics during cyclones are obtained from the Global Positioning System (GPS) Radio Occultation (RO) measurements and ozone and water vapor concentrations in the UTLS region are obtained from Aura-Microwave Limb Sounder (MLS) satellite observations. The effect of cyclones on the tropopause parameters is observed to be more prominent within 500 km from the centre of the tropical cyclone. In our earlier study, we have observed decrease (increase) in the tropopause altitude (temperature) up to 0.6 km (3K) and the convective outflow level increased up to 2 km. This change leads to a total increase in the tropical tropopause layer (TTL) thickness of 3 km within the 500 km from the centre of cyclone. Interestingly, an enhancement in the ozone mixing ratio in the upper troposphere is clearly noticed within 500 km from cyclone centre, whereas the enhancement in the water vapor in the lower stratosphere is more significant on south-east side extending from 500-1000 km away from the cyclone centre. The cross-tropopause mass flux for different intensities of cyclones are estimated and found that the mean flux from the stratosphere to the troposphere for cyclonic storms is $0.05\pm0.29\times10^{-3}$ kgm^{-2} and for very severe cyclonic storms it is $0.5\pm1.07\times10^{-3}$ kgm^{-2}. More downward flux is noticed in the north-west and south-west side of the cyclone centre. These results indicate that the cyclones have significant impact in effecting the tropopause structure, ozone and water vapor budget and consequentially the STE in the UTLS region.

(**Keywords:** Tropical cyclone, tropopause, ozone, water vapor, STE processes.)

1. Introduction

The tropical cyclones with deep convective synoptic scale systems persisting for a few days to week, play an important role on the mass exchange between the troposphere and the stratosphere, and vice versa (Merril, 1998; Emmanuel, 2005). They transport large amount of water vapor, energy and momentum to the upper troposphere and lower stratosphere (UTLS) region (Ray and Rosenlof, 2007). Cyclones provide favorable conditions for entry of the water vapor-rich and ozone-poor air from surface to the lower stratosphere (LS) and dry and ozone-rich air from the LS to the upper troposphere (UT) leading to the stratosphere-troposphere exchange (STE) (Romps and Kuang 2009; Zhan and Wang, 2012; Vogel et al., 2014). These exchanges occur mainly around the tropopause and change the thermal and chemical structure of the UTLS region. The concentration of the water vapor transported from troposphere to stratosphere is controlled by the cold temperatures present at the tropopause and this is a major factor in the STE (Fueglistaler et al., 2009). As a consequence, the STE events play an important role in controlling the ozone in the UTLS region, which will affect the radiation budget of the Earth atmosphere (Intergovernmental Panel on Climate Change, 1996).

Water vapor has major consequences for the radiative balance and heat transport in the atmosphere. Enhanced ozone loss is a secondary effect of increasing water vapor.(Rind and Lonergan, 1995; Forster and Shine, 1999; Dvortsov and Solomon, 2001; Forster and Shine, 2002; Myhre et al., 2007; Intergovernmental Panel on Climate Change, 2007). Even very small changes in lower stratospheric water vapor could affect the surface climate (Riese et al., 2012). Soloman et al. (2010) reported the role of stratospheric water vapor in the global warming.LS water vapor plays an important role on the distribution of ozone in the lower stratosphere (Shindell, 2001). It is important contributor for long-term change in the LS temperatures (Maycock et al., 2014).

In general, most of the air enters into the stratosphere over the tropics (Brewer, 1949;

Dobson, 1956). As suggested by Newell and Gould-Stewart (1981), Bay-of-Bengal (BoB) is

one of the active regions where troposphere air enters into the stratosphere. It is also one of

the active regions for the formation of deep convection associated cyclones which contains

strong updrafts. Earlier studies have shown a close relationship between cyclones and

moistening of the upper troposphere (Wang et al., 1995; Su et al., 2006; Ray and Rosenlof,

2007).

Several studies have been carried out related to water vapor, ozone transport as well

as STE processes around the UTLS region during cyclones. Koteswaram (1967) described

the thermal and wind structure of cyclones in the UTLS region with the major findings of

cold core persisting just above the 15 km and the outflow jets very close to the tropopause.

Penn (1965) reported enchantment in ozone and warmer air situated above the tropopause

over the eye region during hurricane Ginny. Danielsen (1993) reported on troposphere-

stratosphere transport and dehydration in the lower tropical stratosphere during cyclone

period. Baray et al. (1999) studied the STE during cyclone Marlene and they observed

maximum of ozone change at 300 hPa level. Zou and Wu (2005) observed the variations of

columnar ozone in different stages of hurricane by using satellite measurements. Bellevue et

al. (2007) observed increase in ozone concentration in the upper troposphere during Tropical

Cyclone (TC) event. Significant contribution of cyclones on hydration of the UT is reported

by Ray and Rosenlof (2007) and injection of tropospheric air into the low stratosphere due to

overshooting convection by cyclones is reported by Romps and Kuang (2009). Das (2009)

and Das et al. (2016) have studied the stratospheric intrusion into troposphere during the

passage of cyclone by using Mesosphere-Stratosphere-Troposphere (MST) Radar

observations. Strong enhancement of ozone in the upper troposphere is observed during TCs

over BoB (Fadnavis et al., 2011). The increased ozone levels in the boundary layer as well as

96 near surface by as much as 20 to 30 ppbv due to strong downward transport of ozone in the

97 tropical convection is also observed (Betts et al., 2002; Sahu and Lal, 2006; Grant et al.,

98 2008). Cairo et al. (2008) reported that the colder temperatures are observed in the Tropical

99 Tropopause Layer (TTL) region during cyclone Davina and also reported on the impact of the

100 TCs on the UTLS structure and dynamics at the regional scales. A detailed review on the

101 effect of TCs on the UTLS can be found in same report. Recently, Ravindra Babu et al.

102 (2015) reported the effect of cyclones on the tropical tropopause parameters using

103 temperature profile obtained from Constellation Observing System for Meteorology,

104 Ionosphere and Climate (COSMIC) Global Position System Radio Occultation (GPS-RO)

105 measurements. Many studies have been carried out on the role of extra tropical cyclones on

106 the STE (for example Reutter et al., 2015 and references therein) though the quantitative

107 estimates of STE provided by these case studies varied considerably. However, the vertical

108 and horizontal variation of ozone and water vapor in the UTLS region and cross-tropopause

109 flux quantification during cyclones over north Indian Ocean is not well investigated.

110   In the present study, we investigate the spatial and vertical variations of ozone and

111 water vapor in the UTLS region for all the cyclones occurred over north Indian Ocean during

112 2007 to 2013 by using Aura-Microwave Limb Sounder (MLS) satellite observations. The

113 effect of cyclones on the tropopause characteristics is also presented using COSMIC GPS-RO

114 measurements. We also present the cross-tropopause mass flux estimated for each of the

115 cyclones.

116 **2. Data and Methodology**

117   In the present study, we used Aura-MLS water vapor and ozone measurements

118 (version 3.3) provided by the Jet Propulsion Laboratory (JPL). The version 3.3 was released

119 in January 2011 and this updated version has change in the vertical resolution. The vertical

120 resolution of the water vapor is in the range 2.0 to 3.7 km from 316 to 0.22 hPa and along

track horizontal resolution varies from 210 to 360 km for pressure greater than 4.6 hPa. For ozone, vertical resolution is ~2.5 km and the along track horizontal resolution varies between 300 and 450 km (Livesey et al., 2011). The Aura MLS gives around 3500 vertical profiles per day and it crosses the equator at ~1:40 am and ~1:40 pm local time. For calculating the cross-tropopause mass flux, we used ERA-Interim winds obtained during cyclone period.

We have taken the cyclone track information data from India Meteorological Department (IMD) tropical cyclones observed best track data from year 2007-2013. During this period, around 50 cyclones have formed over the north Indian Ocean. Due to the considerable variability of cyclone life-cycles, for the present study we selected only 16 cyclones that lasted for more than 4 days. The tracks of all the cyclones used for the present study are shown in Figure 1. Table 1 shows the classification of the cyclones over the North Indian Ocean. The TCs over the north Indian ocean are classified in to different categories by IMD based on their maximum sustained wind speed. There are classified as : (1) low pressure when the maximum sustained wind speed at the sea surface is < 17 knots (32 km/hr),(2)depression (D) at 17–27 knots (32–50 km/hr), (3) deep depression (DD) at 28–33 knots (51–59 km/hr), (4) cyclonic storm (CS) at 34– 47 knots (60–90 km/hr), (5) severe cyclonic storm (SCS) at 48–63 knots (90–110 km/hr), (6) very severe cyclonic storm (VSCS) at 64–119 knots (119–220 km/hr), and (7) super cyclonic storm (SuCS) at > 119 knots (220 km/hr) (Pattnaik and Rama Rao, 2008). Table 2 shows the different cyclones used in the present study and their maximum intensity, sustained time, and sustained time for peak intensity period of the each cyclone. The mean sustained time for cyclones that occurred during pre-monsoon, monsoon and post-monsoon seasons is 85.5 ± 52.4 hours, 122 ± 46.5 and 112.6 ± 29.47 hours, respectively. Out of the16 cyclones, 4 cyclones (CS-1, SCS-2and VSCS-1)formed during pre-monsoon season, 3 cyclones formed during monsoon season (CS-1, VSCS-1 and SuCS-1) and 9 cyclones (CS-1, SCS-2, and VSCS-6) formed during post-

146   monsoon season (Table 2).Depressions and deep depressions are not considered. The total

147   available MLS profiles for each cyclone that are used in the present study are listed in Table

148   2. We have 94 ± 21 mean MLS profiles for each cyclone used in the present study and when

149   segregated season wise, there are 108 ± 6, 99 ± 21 and 88 ± 23 during monsoon, pre-monsoon

150   and post-monsoon season, respectively. The available total MLS profiles for each cyclone

151   vary with respect to sustained period of the cyclone and overall we have 1517 MLS profiles

152   within 1000 km from the cyclone centre from all the16 cyclones (Figure 2b). Since there are

153   (temporal) limitations in the satellite measurements, mean cross-tropopause flux is estimated

154   only for those cases of the cyclones that lasted for more than 4 days. However, our

155   quantification of the cross-tropopause flux will not be affected by this limitation as earlier

156   studies revealed that the maximum STE occurs during mature to peak stage of cyclone.

157   Details on the selection of 16 cyclones are presented in Ravindra Babu et al. (2015). In Figure

158   1, different colors indicate different categories of the cyclones.

159   **2.1. Tropopause characteristics observed during cyclones**

160   As mentioned earlier, in the tropical region the amount of water vapor transported into

161   the lower stratosphere from the troposphere is controlled by the cold tropical tropopause

162   temperatures (Fueglistaler et al., 2009).Large convection around the eye of the cyclone and

163   strong updrafts near the eye-walls transports large amount of water vapor into the lower

164   stratosphere through the tropopause. In this way, cyclones will affect the tropopause structure

165   (altitude/temperature). Thus, before quantification of STE, we show the tropopause

166   characteristics observed during the TCs. We used post-processed products of level 2 dry

167   temperature profiles with vertical resolution around 200 m provided by the COSMIC Data

168   Analysis and Archival Center (CDAAC) for estimating the tropopause parameters during

169   cyclones period from 2007-2013. COSMIC GPS-RO is a constellation of six microsatellites

170   equipped with GPS receivers (Anthes et al., 2008). We also used CHAllenging Minisatellite

171   Payload (CHAMP) GPS-RO data that are available between the years 2002 to 2006 and

172   COSMIC data from 2007-2013 for getting background climatology of tropopause parameters

173   over the north Indian Ocean.

174   Climatological mean of all the tropopause parameters are obtained by combining

175   GPS-RO measurements obtained from CHAMP and COSMIC (2002-2013). The tropopause

176   parameters include cold-point tropopause altitude (CPH) and temperature (CPT), lapse rate

177   tropopause altitude (LRH) and temperature (LRT) and the thickness of the tropical

178   tropopause layer (TTL), defined as the layer between convective outflow level (COH) and

179   CPH and are calculated for each profile of GPS-RO collected during the above mentioned

180   period. First, we separated the available RO profiles with respect to distance away from the

181   cyclone centre around 1000 km for individual cyclone for each day of the respective cyclone.

182   After separating, we calculated the tropopause parameters as mentioned above for each RO

183   profile. Total number of occultations used in the present study is shown in Figure 2(a). Then

184   we separated the tropopause parameters with respect to the different cyclone intensity. After

185   estimating the tropopause parameters for all the 16 TCs with respect to different intensity,

186   cyclone-centre composite of all tropopause parameters is obtained. After careful analysis, it is

187   found that there is no much variation in the tropopause parameters observed between D and

188   DD, and between CS and SCS, and thus they are combined to DD and CS, respectively. To

189   quantify the effect of the TCs on the tropopause characteristics, the climatological mean is

190   removed from the individual tropopause parameters. The climatological mean tropopause

191   parameters is estimated from the temperature profiles obtained by using GPS-RO data from

192   2002-2013. We also calculated the difference of tropopause parameters for different cyclone

193   intensities (Figures are not shown). Figure 3shows the cyclone centered – composite of mean

194   difference in the tropopause parameters (CPH, LRH, CPT, LRT, COH and TTL thickness)

195   between climatological mean (2002-2013) and individual tropopause parameters observed

196 during cyclones (irrespective of cyclone intensity) and the more detailed results on effect of

197 TCs on the tropopause variations and mean temperature structure in UTLS region during TCs

198 can be found in Ravindra Babu et al. (2015). We have reported that the CPH (LRH) is

199 lowered by 0.6 km (0.4 km) in most of the areas within the 500 km radius from the cyclone

200 centre and the temperature (CPT/LRT) is more or less colder or equal to the climatological

201 values from the area around 1000 km from the cyclone centre. Note that effect of cyclone can

202 be felt up to 2000 km but since the latitudinal variation also comes into picture when we

203 consider 2000 km radius, we restrict our discussion related to variability within 1000 km

204 from the cyclone centre. COH (TTL thickness) has increased (reduced) up to 2 km within 500

205 km from the cyclones and in some areas up to 1000 km. Note that this decrease in TTL

206 thickness is not only because of pushing up of the COH but also due to decrease of CPH.

207 From the above results, we concluded that the tropical tropopause is significantly affected by

208 the cyclones and the effect is more prominent within 500 km from the cyclone centre. These

209 changes in the tropopause parameters are expected to influence water vapor and ozone

210 transport in the UTLS region during cyclones.

211 **3. Results and discussion**

212 **3.1. Ozone variability in the UTLS region during cyclones**

213   To see the variability and the transport of ozone during the passage of cyclones, we

214 investigate the spatial and vertical variability of ozone in the UTLS region using MLS

215 satellite observations. As mentioned in Section 2.1, we also separated the MLS profiles based

216 on the distance from the TC centre for each day of the individual cyclone. From all the 16

217 cyclones cases, we separated the available MLS profiles with respect to distance from the

218 cyclone centre around 1000 km and also we separated the MLS profiles with respect to

219 different intensities of the cyclones. Figure 4shows the normalized cyclone centered –

220 composite of mean ozone mixing ratio (OMR) observed during cyclones (irrespective of

221 cyclone intensity) at 82hPa, 100hPa, 121hPa, and 146 hPa pressure levels during 2007-2013.

222 Note that we have reasonable number of MLS profiles (1517) from 16 cyclones to generate

223 the meaningful cyclone-centre composite of ozone. Black circles are drawn to show distances

224 250 km, 500 km, 750 km and 1000 km away from cyclone center. Since large variability in

225 OMR is noticed from one pressure level to other, we normalized the values to the highest

226 OMR value at a given pressure level. The highest OMR values at 82 hPa, 100 hPa, 121 hPa

227 and 146 hPa pressure levels is 0.38 ppmv, 0.28 ppmv, 0.19 ppmv and 0.13 ppmv,

228 respectively. Large spatial variations in the OMR are observed with respect to the cyclone

229 centre. At 82 hPa, higher OMR (~0.4 ppmv) in the South-West (SW) side up to 1000 km and

230 comparatively low OMR values (~0.2 ppmv) are noticed in the north of the cyclone centre.

231 At 100 hPa, an increase in the OMR (~0.2 ppmv) near the cyclone centre within 500 km is

232 clearly observed. This enhancement in OMR extends up to 146 hPa and is more prominent

233 slightly in the western and eastern side of the cyclone. In general, the large subsidence

234 located at the top of the cyclone centre is expected to bring lower stratospheric ozone to the

235 upper troposphere. This might be the reason for the enhancement of ozone in the cyclone

236 centre within 500 km. Earlier several studies have reported that the intrusion of the

237 stratospheric air in to the troposphere due to the subsidence in the eye region (Penn, 1965;

238 Baray et al., 1999; Das et al., 2009; Das et al., 2015). The present results also support this

239 aspect that the detrainment of ozone reached to the 146 hPa might be due to strong

240 subsidence. Interestingly, an enhancement in OMR in south east side at 121 hPa but not

241 either at 100 hPa or at 146 hPa can be noticed which need to be investigated further. Thus, in

242 general, higher ozone concentrations are observed in cyclone centre within 500 km and

243 slightly aligned to the western side of the cyclone centre.

244   In order to quantify the impact of cyclones on UTLS ozone more clearly we have

245 obtained anomalies by subtracting the mean cyclone-centered ozone observed during

246 cyclones from the background climatology of UTLS ozone that is calculated by using the

247 total available MLS profiles from 2007-2013. Figure 4(e-h) shows the normalized mean

248 difference of cyclone-centered ozone obtained after removing the background climatology

249 values for different pressure levels shown in Figure 4(a-d). The maximum difference in OMR

250 for corresponding normalized value at 82 hPa, 100 hPa, 121 hPa and 146 hPa pressure levels

251 is -0.089 ppmv, -0.19 ppmv, -0.09 ppmv and -0.06 ppmv, respectively. Enhancement in the

252 OMR (~0.1 ppmv) up to 1000 km from the cyclone centre is observed at 82 hPa.

253 Interestingly, at 100 hPa OMR is more or less uniform throughout 1000 km from the cyclone

254 centre except ~500 km radius from the centre where significant increase of OMR (~0.2

255 ppmv) is observed. This increase in the OMR is within 500 km from cyclone centre and

256 extends up to 121 hPa. However, enhancement in OMR at 146 hPa extends up to 1000 km

257 but distributed towards eastern and western sides of cyclone centre. Thus, it is clear that the

258 detrainment of lower stratospheric ozone will reach up to 146 hPa during cyclone period due

259 to presence of strong subsidence in the cyclone centre. We also calculated the cyclone-centre

260 composite of ozone based on different cyclone intensities such as DD, SCS and VSCS. After

261 carefully going through them, we have found that this detrainment of ozone reaching up to

262 146 hPa is more in the higher intensity period of the TCs. We do not know what happens

263 below this pressure level due to limitation in the present data, however, studies (Das et al.,

264 2015; Jiang et al., 2015) have shown that LS ozone can reach as low as boundary layer during

265 cyclones. It will be interesting to see the variability in the water vapor as large amount of it is

266 expected to cross the tropopause during the cyclone period and reach lower stratosphere.

267 **3.2. Water vapor variability in the UTLS region during cyclones**

268   As mentioned earlier, enormous amount of water vapor is expected to be pumped

269 from lower troposphere to the upper troposphere and even it can penetrate into the lower

270 stratosphere during cyclones. To see the linkage between tropopause variability and the

271 transport of water vapor during cyclones, we investigated the horizontal and vertical

272 variability of water vapor in the UTLS region using MLS satellite observations. Figure

273 5shows the normalized cyclone centered – composite of mean water vapor mixing ratio

274 observed during cyclones (irrespective of cyclone intensity) at 82hPa, 100hPa, 121hPa, and

275 146 hPa pressure levels observed by MLS during 2007-2013. Black circles are drawn to

276 shown the 250 km, 500 km, 750 km and 1000 km away from cyclone center. The highest

277 Water Vapor Mixing Ratio (WVMR)values for corresponding normalized value at 82 hPa,

278 100 hPa, 121 hPa, and 146 hPa pressure levels is 4.44 ppmv, 4.49 ppmv, 6.9 ppmv and 16.03

279 ppmv, respectively. Significantly higher WVMR values are noticed extending from 500 km

280 up to 1000 km from the cyclone centre at 121 (~6.5 ppmv), 146 hPa (~15 ppmv) levels with

281 more prominence in the eastern side of the cyclon ecentre. Comparatively low values are

282 noticed in the centre of the cyclone, especially at 121 hPa. These results are comparing well

283 with higher WVMR observed in the eastern side of cyclones over Atlantic and Pacific Oceans

284 (Ray and Rosenlof, 2007). These results also compare well with those reported by Ravindra

285 Babu et al. (2015) where they used GPS-RO measured relative humidity and found

286 enhancement in RH in the eastern side of the centre in the upper troposphere (10-15 km) over

287 north Indian Ocean. The higher WVMR values are observed in the eastern side of the cyclone

288 centre might be due to the upper level anti-cyclonic circulation over the cyclones. It is

289 interesting to note that high WVMR lies not at the centre but extend from 500 to 1000 km

290 from the centre of cyclone. The WVMR show high at 121 and 146 hPa than at 100 and 82

291 hPa. It seems less water vapor has been transported to 100 and 82 hPa from below. As we

292 know, water vapor mostly origin from lower troposphere and decreasing with height. So

293 vertical transport of water vapor from the lower troposphere to the UTLS may lead to water

294 vapor enhanced at 121 and 146 hPa and some time it reaches to higher altitudes. The higher

295 WVMR presented at 100 and 82 hPa levels show the signature of the tropospheric air

296 entering even in to the lower stratosphere during cyclones.

297 In order to quantify the impact of cyclones on the UTLS water vapor more clearly, we

298 have obtained anomalies by subtracting the mean cyclone-centered water vapor observed

299 during cyclones from the background climatology mean of UTLS water vapor. Figure 5(e-h)

300 shows the normalized mean difference of the cyclone-centered WVMR obtained after

301 removing the background climatology values for different pressure levels shown in Figure

302 5(a-d). The maximum difference in WVMR for corresponding normalized values at 82 hPa,

303 100 hPa, 121 hPa, and 146 hPa pressure levels is -0.44 ppmv, -0.81 ppmv, -2.55 ppmv and -

304 9.09 ppmv, respectively. More than 7 ppmv differences are observed at 146 hPa within the

305 1000 km from the centre and at 121 hPa difference of ~ 2 ppmv is noticed extending up to

306 2000 km (figure not shown) in the eastern side of the centre. At 100 hPa and 82 hPa levels,

307 the increase in the WVMR is ~0.8 and ~0.6 ppmv, respectively, and the enhancement is more

308 observed in the NE side of the cyclone centre. Thus, a clear STE is evident during the

309 cyclone over north Indian Ocean where a clear enhancement in the water vapor (ozone) in the

310 lower stratosphere (upper troposphere) is observed. For quantifying the amount of STE, we

311 calculated the cross-tropopause mass flux for each cyclone by considering the spatial extent

312 within the 500 km from the cyclone centre and results are presented in the following sub-

313 section.

314 **3.3. Cross tropopause flux observed during cyclones**

315 We adopted method given by Wei (1987) to estimate the cross tropopause mass flux,

316 *F*. *F* is defined as:

317 $$F = \frac{1}{g}\left(-\omega + V_h.\nabla P_{tp} + \frac{\partial P_{tp}}{\partial t}\right) = \left(-\frac{\omega}{g} + \frac{1}{g}V_h.\nabla P_{tp}\right) + \frac{1}{g}\frac{\partial P_{tp}}{\partial t} = F_{AM} + F_{TM} \qquad (1)$$

318   where ω is the vertical pressure-velocity, V_h is the horizontal vector wind, P_{tp} is the pressure

319   at the tropopause, g is the acceleration due to gravity, F_{AM} is the air mass exchange due to

320   horizontal and vertical air motions, F_{TM} is the air mass exchange due to tropopause motion.

321   The wind information is taken from ERA-Interim, and the tropopause temperature and

322   pressure within 500 km from the cyclone centre is estimated from COSMIC GPS-RO

323   measurements (Ravindra Babu et al., 2015). These values are considered for the maximum

324   intensity day for each of the 16 cyclones and the respective cross tropopause flux is

325   estimated. Since the above mentioned results showed that the higher OMR values are

326   observed in the west and NW side and more water vapor is located at the eastern side of the

327   cyclone centre, we separated the area into 4 sectors with respect to cyclone centre as C1 (NW

328   side), C2 (NE side), C3 (SW side), and C4 (SE side), respectively as shown in Figure 4(a).

329   List of cyclones used in the present study with their names, cyclone intensity (CI), centre

330   latitude, centre longitude, minimum estimated central pressure on their peak intensify day are

331   provided in Table 3. The total flux F (equation 1) depends on the air mass exchange due to

332   horizontal and vertical air motion (F_{AM}), and the air mass exchange due to tropopause motion

333   itself (F_{TM}). Since number of COSMIC GPS-RO measurements are not sufficient to estimate

334   the second term (F_{TM}) for each event, we calculated only the first part of the equation (F_{AM})

335   individually for each of cyclone with respect to different sectors mentioned above and the

336   values are presented in Table 3.However, we roughly estimated the contribution of second

337   term by assuming change in the tropopause pressure by 0.5 hPa increase (decrease) within 6

338   hr and could see cross-tropopause flux for CS is $0.25\pm0.07 \times 10^{-3}$ $kgm^{-2}s^{-1}$ ($-0.36\pm0.07\times10^{-3}$

339    $kgm^{-2}s^{-1}$) and for VSCS it is $-0.24\pm0.3\times10^{-3}$ $kgm^{-2}s^{-1}$ ($-0.85\pm0.3\times10^{-3}$ $kgm^{-2}s^{-1}$). If there is

340   change in the tropopause pressure by 1 hPa increase (decrease), the flux for CS is

341    $0.55\pm0.07\times10^{-3}$ $kgm^{-2}s^{-1}$ ($-0.66\pm0.07\times10^{-3}$ $kgm^{-2}s^{-1}$) and for VSCS it is $0.06\pm0.3\times10^{-3}$ $kgm^{-2}s^{-1}$

342   ($-1.16\pm0.3\times10^{-3}$ $kgm^{-2}s^{-1}$).

343   Figure 6shows the cross-tropopause flux estimated in each sector from the centre of

344   the cyclone for the different cyclone intensities (estimated based on the cyclone centre

345   pressure). Red lines show the best fit. It clearly shows that the downward flux is always more

346   in C1 and C3 sectors, whereas C2 sector show more upward flux. The flux itself varies with

347   the cyclone intensity and it is found that the increase in downward flux as the cyclone centre

348   pressure decreases particularly forC1 and C3 sectors. Whereas, in C4 sector, increase in the

349   upward flux is seen as the cyclone intensity increases but always upward in C2 sector,

350   irrespective of the cyclone intensity. The second term (in equation 1) itself corresponds the

351   air mass exchange from the tropopause motion and generally during cyclone period there is

352   an ~400 m difference in tropopause altitude (LRH) within 500 km from the centre of the

353   cyclone (Figure 3).Thus, the spatial and temporal variation of the tropopause during the

354   cyclones itself is very important for to decide the flux as downward or upward. Interestingly,

355   C1 and C3 sectors of cyclone show dominant downward mean flux and C2 and C4 sectors

356   show dominant upward mean flux with the values of $0.4\pm0.4\times10^{-3}$kgm^{-2}, $1.2\pm1.0\times10^{-3}$kgm^{-2},

357    $0.2\pm0.1\times10^{-3}$ kgm^{-2}and $0.12\pm0.3\times10^{-3}$ kgm^{-2}, respectively. These results strongly support our

358   findings of higher ozone in the NW and SW sides and higher water vapor in the NE side of

359   the cyclone centre. The mean flux is observed to vary with the intensity of the cyclone. Mean

360   flux for the severe cyclonic storms (CS) is $-0.05\pm0.29\times10^{-3}$ kgm^{-2}whereas for very severe

361   cyclonic storms (VSCS) it is $-0.5\pm1.07\times10^{-3}$kgm^{-2}. Reutter et al. (2015) reported the upward

362   and downward mass fluxes across the tropopause are more dominant in a deeper cyclones

363   compared to a less intense cyclones over the North Atlantic. Our results are comparable with

364   their results with the averaged mass flux of the stratosphere to troposphere as 0.3×10^{-3} kgm^{-2}

365   s^{-1} (340 kgkm^{-2} s^{-1}) in the vicinity of cyclones over the North Atlantic Ocean. They also

366   reported that the more transport across the tropopause occurred in the west side of the

367 cyclone centre during intensifying and mature stages of the cyclones over the North Atlantic

368 region.

369 **4. Summary and conclusions**

370   In this study, we have investigated the vertical and spatial variability of ozone and

371 water vapor in the UTLS region during the passage of cyclones occurred between 2007 and

372 2013 over the North Indian Ocean by using Aura-MLS satellite observations. In order to

373 make quantitative estimate of the impact of cyclones on the ozone and water vapor budget in

374 the UTLS region, we removed the mean cyclone-centre ozone and water vapor from the

375 climatological mean calculated using MLS data from 2007 to 2013. We estimated the mean

376 cross- tropopause flux for each of the cyclones on their peak intensity day. The main findings

377 are summarized below.

378   1. Lowering of the CPH (0.6 km) and LRH (0.4 km) values with the coldest CPT and

379   LRT (2–3 K) within a 500 km radius from the cyclone centre is noticed. Higher (2

380   km) COH leading to the lowering of TTL thickness (~3 km) is clearly observed

381   (Ravindra Babu et al., 2015).

382   2. The impact of cyclones on ozone and the tropopause (altitude/temperature) is more

383   prominent within 500 km from the cyclone centre, whereas it is high from 500 km to

384   1000km in case of water vapor.

385   3. Detrainment of ozone is highest in the cyclone centre (within 500 km from the centre)

386   due to strong subsidence over top of the cyclone centre and this detrained ozone

387   reaches as low as 146 hPa level (~13-14 km).

388   4. The detrainment of ozone is more in the higher intensity period (SCS or VSCS) of the

389   cyclone compared to the low intensity (D or DD).

390   5. Interestingly, significant enhancement in the lower stratospheric (82 hPa) water vapor

391   is noticed in the east and southeast side from the cyclone centre.

392   6. Dominant downward [upward] cross-tropopause flux is observed in C1 (NW) and C3

393   (SW) [C2 (NE) and C4 (SE)] sectors of the cyclone.

394   Figure 7 shows the typical structure (not to scale) of the TC along with convective towers,

395   updrafts, downdrafts which above mentioned tropopause variability with respect to cyclone

396   centre in the form of the schematic diagram. The tropopause altitude (CPH) is lowered by

397   0.6 km within 500 km from the centre of the cyclone. The convective out flow level (COH)

398   slightly pushes up (~2 km) with in 500 km from the centre of the cyclone but not exactly in

399   the centre. Thus, a decrease of about 3 km in the TTL thickness is observed within the 500

400   km from the cyclone centre. Cyclone includes eye that extends from few km to 10's of

401   kilometers. Strong convective towers with strong updrafts extending up to the tropopause in

402   the form of spiral bands extending from 500 to 1000 km are present. Strong water vapor

403   transport in to the lower stratosphere (82 hPa) while pushing up the COH is observed around

404   these spiral bands in the present study. Between these spiral bands equal amount of

405   subsidence is expected with strong subsidence existing at the centre of the cyclone.

406   Significant detrainment of ozone present above or advected from the surroundings is

407   observed reaching as low as 146 hPa at the cyclones centre. Thus, it is clear that ozone

408   reaches upper troposphere from lower stratosphere through the centre of the cyclone, whereas

409   water vapor transport in to the lower stratosphere will happen from the 500 to 1000 km from

410   the cyclones centre. Since more intense cyclones are expected to occur in a changing climate

411   (Kuntson et al., 2010), the amount of water vapor and ozone reaching to the lower

412   stratosphere and upper troposphere, respectively, is expected to increase thus affecting

413   complete tropospheric weather and climate. Future studies should focus on these trends.

414   **Acknowledgements:** We would like to thank COSMIC Data Analysis and Archive Centre

415   (CDAAC) for providing GPS-RO data used in the present study through their FTP site

416   (http://cdaac-www.cosmic.ucar.edu/cdaac/products.html). The provision of tropical cyclone

417 best track data used in the present study by IMD through their website
418 (http://www.imd.gov.in/section/nhac/dynamic/cyclone.htm) and Aura-MLS observations
419 obtained from the GES DISC through their ftp site (https://mls.jpl.nasa.gov/index-eos-
420 mls.php) is highly acknowledged. This work is supported by Indian Space Research
421 Organization (ISRO) through CAWSES India Phase-II Theme 3programme. The authors
422 would like to thank the Editor Dr. Rolf Müller, and two anonymous reviewers whose
423 comments helped considerably in improving the quality of this paper

424

References:

Anthes, R. A., Bernhardt, P. A., Chen, Y., Cucurull, L., Dymond, K. F., Ector, D., Healy, S. B., Ho, S.-H., Hunt, D. C., Kuo, Y.-H., Liu, H., Manning, K., McCormick, C., Meehan, T. K., Randel, W. J., Rocken, C., Schreiner, W. S., Sokolovskiy, S. V., Syndergaard, S., Thompson, D. C., Trenberth, K. E., Wee, T.-K., Yen, N. L., and Zeng, Z.: The COSMIC/Formosat/3 mission: Early results, B. Am. Meteorol. Soc., 89, 313–333, 2008.

Baray, J. L., Ancellet, G., Radriambelo T., and Baldy, S.: Tropical cyclone Marlene and stratosphere-troposphere exchange, J. Geophys. Res., 104, 13,953–13,970, doi:10.1029/1999JD900028-1999.

Bellevue, J., Baray, J. L., Baldy, S., Ancellet, G., Diab, R. D., and Ravetta, F.: Simulations of stratospheric to tropospheric transport during the tropical cyclone Marlene event, Atmos. Environ., 41, 6510–6526, doi:10.1016/j.atmosenv.2007.04.040, 2007.

Betts, A. K., Gatti, L. V., Cordova, A. M., Silva Dias, M. A. F., and Fuentes, J. D.: Transport of ozone to the surface by convective downdrafts at night, J. Geophys. Res., 107, 8046, doi:10.1029/2000JD000158, 2002.

Brewer, A. W.: Evidence for a world circulation provided by the measurements of helium and water vapor distribution in the stratosphere.Quarterly Journal of Royal Meteorological Society., 75, 351–363, doi:10.1002/qj.49707532603-1949.

Cairo, F., Buontempo, C., MacKenzie, A. R., Schiller, C., Volk, C. M., Adriani, A., Mitev, V., Matthey, R., Di Donfrancesco, G., Oulanovsky, A., Ravegnani, F., Yushkov, V., Snels, M., Cagnazzo, C., and Stefanutti, L.: Morphology of the tropopause layer and lower stratosphere above a tropical cyclone: a case study on cyclone Davina (1999), Atmos. Chem. Phys., 8, 3411– 3426, doi:10.5194/acp-8-3411-2008, 2008.

Danielsen, E. F.: In situ evidence of rapid, vertical, irreversible transport of lower tropospheric air into the lower tropical stratosphere by convective cloud turrets and by

larger-scale upwelling in tropical cyclones, J. Geophys. Res., 98, 8665–8681, doi: 10.1029/92JD02954-1993.

Das, S. S.: A new perspective on MST radar observations of stratospheric intrusions into troposphere associated with tropical cyclone. Geophys. Res. Lett., 36, L15821, doi: 10.1029/2009GL039184-2009.

Das, S.S., Ratnam, M. V., Uma, K.N., Subrahmanyam, K.V., Girach, I.A., Patra, A.K., Aneesh, S., Suneeth, K.V., Kumar, K.K., Kesarkar, A.P., Sijikumar, S., and Ramkumar, G.: Influence of Tropical Cyclone on Tropospheric Ozone: Possible Implication, Atmos. Chem. Phys. Discuss., 15, 19305-19323, 2015.

Das, S.S., Ratnam, M.V., Uma, K. N., Patra, A. K., Subrahmanyam, K. V., Girach, I. A., Suneeth, K.V., Kumar, K. K., and Ramkumar, G.: Stratospheric intrusion into the troposphere during the tropical cyclone Nilam (2012), Q. J. Royal Meteo. Soc., doi: 10.1002/qj.2810, 2016.

Dobson, G. M. B.: Origin and Distribution of the Polyatomic Molecules in the Atmosphere, Royal Society of London Proceedings Series A, 236, 187–193, doi:10.1098/rspa.1956.0127, 1956.

Dvortsov, V. L., and Solomon, S.: Response of the stratospheric temperatures and ozone to past and future increases in stratospheric humidity, J. Geophys. Res., 106, 7505 – 7514, 2001.

Emanuel, K. A.: Increasing destructiveness of tropical cyclones over the past 30 years, Nature, 436, 686–688, doi:10.1038/nature03906, 2005.

Fadnavis, S., Berg, G., Buchunde, P., Ghude, S. D., and Krishnamurti, T. N.: Vertical transport of ozone and CO during super cyclones in the Bay of Bengal as detected by Tropospheric Emission Spectrometer, Environ. Sci. Pollut. R., 18, 301–315, doi:10.1007/s11356-010-0374-3, 2011.

475   Forster, P.M. de F., and Shine, K. P.: Stratospheric water vapour changes as a possible

476   contributor to observed stratospheric cooling, Geophys. Res. Lett., 26, 3309-3312, 1999.

477   Forster, P. M. And Shine, K. P.: Assessing the climate impacts of trends in stratospheric

478   water vapour. Geophys. Res. Lett. 29: 1086–1089, doi: 10.1029/2001GL013909-2002.

479   Fueglistaler, S., Dessler, A. E., Dunkerton, T. J., Fu, I., Folkins, Q., and Mote, P. W.:

480   Tropical tropopause layer, Rev. Geophys., 47, RG1004, doi:10.1029/2008RG000267, 2009.

481   Grant, D. D., Fuentes, J. D., DeLonge, M. S., Chan, S., Joseph, E., Kucera, P., Ndiaye, S. A.,

482   and Gaye, A. T.: Ozone transport by mesoscale convective storms in western Senegal,

483   Atmos. Environ., 42, 7104–7114, doi:10.1016/j.atmosenv.2008.05.044, 2008.

484   IPCC 1996: IPCC, Climate Change 1995 – The Science of Climate Change, Contribution of

485   Working Group I to the Second Assessment Report, section 2 edited by: Houghton, J. T.,

486   MeiraFilho, L. G., Callander, B. A., Harris, N., Kattenberg, A., and Maskell, K., University

487   Press, Cambridge, 572 pp., 1996.

488   Jiang, Y.C., Zhao, T.L., Liu, J., Xu, X.D., Tan, C.H., Cheng, X.H., Bi, X.Y., Gan, J.B., You,

489   J.F., andZhao, S.Z.: Why does surface ozone peak before a typhoon landing in

490   southeastChina?Atmos. Chem. Phys., 15, 13331–13338, 2015

491   Koteswaram, P.: On the structure of hurricanes in the upper troposphere and lower

492   stratosphere, Mon. Weather Rev., 95, 541–564, 1967.

493   Knutson, T.R., John,L.. McBride, Johnny Chan, Kerry Emanuel, Greg Holland, Chris

494   Landsea, Isaac Held, James P. Kossin, Srivastava, A.K., and Masato Sugi: Tropical

495   cyclones and climate change, Nature Geosci., 3, 157 – 163, 2010.

496   Livesey, N., Read, W. G., Frovideaux, L., Lambert, A., Manney, G. L., Pumphrey, H. C.,

497   Santee, M. L., Schwartz, M. J., Wang, S., Cofield, R. E., Cuddy, D. T., Fuller, R. A.,

498   Jarnot, R. F., Jiang, J. H., Knosp, B. W., Stek, P. C., Wagner, P. A., and Wu, D. L.: Earth

Observing System (EOS) Aura Microwave Limb Sounder (MLS) Version 3.3 Level 2 data

quality and description document, JPL D-33509, JPL publication, USA, 2011.

Maycock, A. C., Joshi, M.M., Shine,K.P., Davis,S.M and Rosenlof,K.H.: The potential

impact of changes in lower stratospheric water vapour on stratospheric temperatures over

the past 30 years. Quart. J. Roy. Meteor. Soc., 140, 2176–2185, doi:10.1002/ qj.2287-

2014.

Merrill, R. T. (1988), Characteristics of the upper-tropospheric environmental flow around

hurricanes, J. Atmos. Sci., 45, 1665–1677, doi:10.1175/ 1520

0469(1988)045<1665:COTUTE>2.0.CO;2.

Myhre, G., Nilsen, J. S., Gulstad, L., Shine, K. P., Rognerud, B., and Isaksen, I. S. A.:

Radiative forcing due to stratospheric water vapour from CH4 oxidation, Geophys. Res.

Lett., 34, L01807, doi:10.1029/2006gl027472, 2007.

Newell, R. E., and Gould-Stewart, S.: A stratospheric fountain, Journal of Atmospheric

Science., 38, 2789–2796, doi:10.1175/1520-0469-1981.

Pattnaik, D. R. and Rama Rao, Y. V.: Track Prediction of very sever cyclone "Nargis" using

high resolution weather research forecasting (WRF) model, J. Earth Syst. Sci., 118, 309–

329, 2008.

 Penn, S.: Ozone and temperature structure in a Hurricane, J. Appl. Meteorol., 4, 212–216,

1965.

Ravindra Babu,S., Venkat Ratnam, M., Basha, G., Krishnamurthy. B.V. and Venkateswara

Rao, B.: Effect of tropical cyclones on the tropical tropopause parameters observed using

COSMIC GPS RO data. Atmos. Chem. Phys., 15, 10239-10249, doi: 10.5194/acp-15-

10239-2015.

Ray, E. A. and Rosenlof, K. H.: Hydration of the upper troposphere by tropical cyclones, J.

Geophys. Res., 112, D12311, doi:10.1029/2006JD008009, 2007.

524   Reutter, P., Škerlak, B., Sprenger, M., and Wernli, H.: Stratosphere-troposphere exchange

525   (STE) in the vicinity of North Atlantic cyclones. Atmos. Chem. Phys., 15, 10939–10953,

526   2015.

527   Riese, M., F. Ploeger, A. Rap, B. Vogel, P. Konopka, M. Dameris, and Forster, P.: Impact of

528   uncertainties in atmospheric mixing on simulated UTLS composition and related radiative

529   effects, J. Geophys. Res., 117, D16305, doi:10.1029/2012JD017751-2012.

530   Rind, D., and Lonergan,. P.: Modeled impacts of stratospheric ozone and water vapor

531   perturbations with implications for high-speed civil transport aircraft. *J. Geophys.*

532   *Res.*, 100, 7381-7396, doi:10.1029/95JD00196- 1995.

533   Romps, D. M. and Kuang, Z. M.: Overshooting convection in tropical cyclones, Geophys.

534   Res. Lett., 36, L09804, doi:10.1029/2009GL037396, 2009.

535   Sahu, L. K. and Lal, S.: Changes in surface ozone levels due to convective downdrafts over

536   the Bay of Bengal, Geophys. Res. Lett., 33, L10807, doi:10.1029/2006GL025994, 2006.

537   Shindell, D.T.: Climate and ozone response to increased stratospheric water vapor. Geophys.

538   Res. Lett. 28, 1551-1554, 2001.

539   IPCC, 2007a: Climate Change 2007: The Physical Science Basis. Contribution of Working

540   Group I to the Fourth Assessment Report of the Intergovernmental Panel on Climate

541   Change [Solomon, S., D. Qin, M. Manning, Z. Chen, M. Marquis, K.B.M.Tignor and H.L.

542   Miller (eds.)]. Cambridge University Press, Cambridge, United Kingdom and New York,

543   NY, USA, 996 pp.

544   Solomon, S., Rosenlof, K. H., Portmann, R. W., Daniel, J. S., Davis, S. M., Sanford, T. J.,

545   and Plattner, G.-K.: Contributions of Stratospheric Water Vapor to Decadal Changes in the

546   Rate of Global Warming, Science, 327, 1219–1223, 2010.Stenke, A. and Grewe, V.:

547   Simulation of stratospheric water vapor trends: impact on stratospheric ozone chemistry.

548   Atmos. Chem. Phys., 5, 1257–1272, doi: 10.5194/acp-5-1257-2005.

549   Su, H., Read, W.G., Jiang, J. H., Waters, J. W., Wu, D. L., and Fetzer, E. J.: Enhanced

550   positive water vapor feedback associated with tropical deep convection: New evidence

551   from Aura MLS. Geo. Research Letters., 33, L05709, doi: 10.1029/2005GL025505-2006.

552   Vogel, B., Günther, G., Müller, R., Grooß, J.-U., Hoor, P., Krämer, M., Müller, S., Zahn, A.,

553   and Riese, M.: Fast transport from Southeast Asia boundary layer sources to northern

554   Europe: rapid uplift in typhoons and eastward eddy shedding of the Asian monsoon

555   anticyclone, Atmos. Chem. Phys., 14, 12745-12762, doi:10.5194/acp-14-12745-2014,

556   2014.

557   Wei, M. Y.: A new formulation of the exchange of mass and trace constituents between the

558   stratosphere and troposphere. Journal of Atmospheric Science., 44(20), 3079–3086,

559   doi:10.1175/1520-0469-1987.

560   Zhan, R. and Wang, Y.: Contribution of tropical cyclones to stratosphere–troposphere

561   exchange over the northwest Pacific: estimation based on AIRS satellite retrievals and

562   ERA-Interim data, J. Geophys. Res., 117, D12112, doi: 10.1029/2012.

563   Zou, X., and Y. Wu.: On the relationship between Total Ozone Mapping Spectrometer

564   (TOMS) ozone and hurricanes. J. Geophys. Res.,110, D06109, doi:

565   10.1029/2004JD005019-2005.

 Figure captions:

 Figure 1. Tropical cyclone tracks of different categories (cyclonic storm (CS, blue color),

    severe cyclonic storm (SCS, orange color), very severe cyclonic storm (VSCS, red color)

    and super cyclonic storm (SuCs, magenta color)) that occurred over North Indian Ocean

    during 2007 - 2013.

 Figure 2. Cyclone-centred composite of total available (a) COSMIC GPS RO occultations

    and (b) MLS profiles obtained from all the 16 cyclones that are used in the present study.

 Figure 3. Cyclone centered – composite of mean difference in the tropopause parameters

    between climatological mean (2002-2013) and individual tropopause parameters observed

    during cyclones(irrespective of cyclone intensity) in (a) CPH (km), (b) LRH (km), (c) CPT

    (K), (d) LRT (K), (e) COH (km) and (f) TTL thickness (km). Black circles are drawn to

    show the 250 km, 500 km, 750 km and 1000 km away from cyclone center.

 Figure 4. Normalized cyclone centered – composite of mean ozone mixing ratio observed

    during cyclones (irrespective of cyclone intensity) at (a) 82hPa, (b) 100hPa, (c) 121hPa, (d)

    146 hPa levels by MLS during 2007-2013. (e) to (h) same as (a) to (d) but for normalized

    mean difference in the ozone mixing ratio between climatological mean (2007-2013) and

    individual events. Black circles are drawn to show the 250 km, 500 km, 750 km and 1000

    km away from cyclone center. Sectors showing C1 (NW), C2 (NE), C3 (SW) and C4 (SE)

    are also shown in (a).

 Figure 5. Same as Fig. 4, but for water vapor mixing ratio.

 Figure 6. Cross-tropopause flux estimated in the (a) C1 (NW), (b) C2 (NE), (c) C3 (SW), and

    (d) C4 (SE) sectors from the centre of cyclone for different cyclone intensities (estimated

    based on cyclone centre pressure). Red lines show the best fit.

 Figure 7. Schematic diagram showing the variability of CPH (brown color line) and COH

    (magenta color line) with respect to the centre of cyclone. Spiral bands of convective

591   towers reaching as high as COH are shown with blue color lines. Light blue (red) color up

592   (down) side arrow shows the up drafts (downdrafts/subsidence). Thickness of the arrows

593   indicates the intensity.

594

595   **Table captions:**

596   **Table1**.Classification of cyclonic systems over the north Indian Ocean.

597   **Table 2.** Tropical cyclones occurred during different seasons, cyclone name, cyclone

598   Intensity (CI), cyclone period, total sustained time, Sustained time with maximum intensity

599   and total number of available MLS profiles

600   **Table 3.** Cyclone name, cyclone Intensity (CI), centre latitude, centre longitude, estimated

601   central pressure and estimated cross-tropopause mass flux with respect to cyclone centre

602   for C1 (NW side), C2 (NE side), C3 (SW side) and C4 (SE side), respectively.

603

604 **Tables:**

605 **Table1.**IMD classification of cyclonic systems over the north Indian Ocean.

Intensity of the system	Maximum sustained surface winds (knots) at sea (1 knot =0.5144 m/s)
Low pressure area	<17
Depression	17–27
Deep depression (DD)	28–33
Cyclonic storm (CS)	34-47
Severe cyclonic storm (SCS)	48-63
Very severe cyclonic storm (VSCS)	64–119
Super cyclonic storm (SuCS)	>119

606

607

608

609

610

611

612

613

614

615

616

617

618 **Table 2.** Tropical cyclones occurred during different seasons, cyclone name, cyclone

619 Intensity (CI), cyclone period, total sustained time, Sustained time with maximum intensity

620 and total number of available MLS profiles.

Season	Cyclone Name	Cyclone Intensity (CI)	Cyclone Period (days)	Total Sustained time (hours)	Sustained Time with maximum intensity (hours)	Total available MLS profiles
Monsoon (JJA)	03B(2007)	CS	>4	75	6	104
	PHET (2010)	VSCS	>4	168	42	116
	Gonu (2007)	ScCS	>4	123	72	105
Pre-Monsoon (MAM)	Mahasen(2013)	CS	>4	24	24	119
	Aila (2009)	SCS	4	72	9	79
	Laila (2010)	SCS	4	96	27	82
	Nargis (2008)	VSCS	>4	150	87	118
Post-Monsoon (SON)	Nilam (2012)	CS	>4	102	36	52
	Jal (2010)	SCS	4	99	30	75
	Helen (2013)	SCS	4	78	30	72
	Giri (2010)	VSCS	4	66	15	65
	Phailin (2013)	VSCS	>4	147	66	111
	Leher (2013)	VSCS	>4	114	36	111
	SIDR (2007)	VSCS	>4	138	72	114
Winter (DJF)	Madi (2013)	VSCS	>4	150	36	104
	Thane (2011)	VSCS	>4	120	36	90

621

622

623

624 **Table 3.** Cyclone name, cyclone Intensity (CI), centre latitude, centre longitude, estimated

625 central pressure and estimated cross-tropopause mass flux with respect to cyclone centre

626 for C1 (NW side), C2 (NE side), C3 (SW side) and C4 (SE side), respectively.

627

					Flux @500km			
Cyclone	CI	Centre Latitude	Centre Longitude	Estimated Central Pressure (hPa)	C1	C2	C3	C4
03B	CS	23.5	66	986 (25Jun2007)	-0.013	0.661	-0.603	-0.258
Aila	SCS	22	88	968 (25May2009)	1.90E-04	0.191	-0.299	-0.072
Helen	SCS	16.1	82.7	990 (21Nov2013)	0.025	0.216	-0.095	-0.11
Jal	SCS	11	84	988(6Nov2010)	0.025	0.384	-0.4	-0.218
Laila	SCS	14.5	81	986 (19May2010)	-0.012	0.123	-0.352	-0.299
Mahasen	CS	18.5	88.5	990 (15May2013)	-0.006	0.354	-0.473	-0.256
Nilam	CS	11.5	81	990 (31Oct2012)	0.016	0.313	-0.274	-0.097
Nargis	VSCS	16	94	962 (2May2008)	-0.828	0.094	-1.946	0.384
Giri	VSCS	19.8	93.5	950 (22Oct2010)	-0.518	0.022	-0.823	0.032
Gonu	SuCS	20	64	920 (4Jun2007)	-0.502	0.123	-2.563	0.37
Lehar	VSCS	13.2	87.5	980 (26Nov2013)	-0.55	0.119	-2.019	0.411
Madi	VSCS	13.4	84.7	986 (10Dec2013)	-0.375	0.054	-1.449	0.352
Phailin	VSCS	18.1	85.7	940 (11Oct2013)	-0.9	0.179	-2.576	0.479
Phet	VSCS	18	60.5	964 (2Jun2010)	-1.058	0.203	-2.698	0.559
SIDR	VSCS	19.5	89	944 (15Nov2007)	-0.493	0.066	-0.926	0.231
Thane	VSCS	11.8	80.6	970 (29Dec2011)	-1.272	0.356	-2.979	0.558

628

629

630 **Figures:**

631
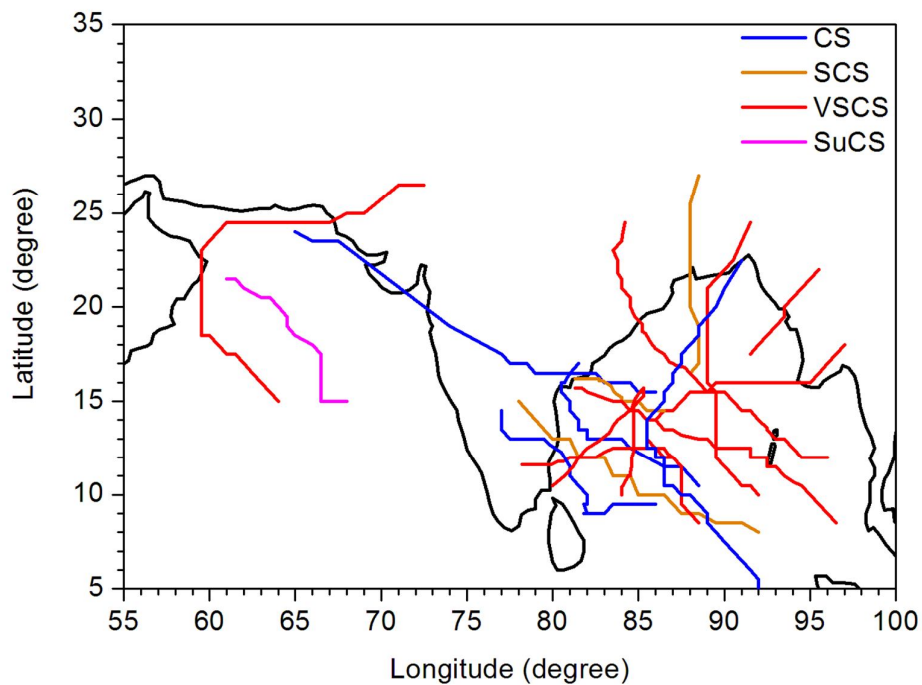
632

633 **Figure 1.** Tropical cyclone tracks of different categories (cyclonic storm (CS, blue color),

634 severe cyclonic storm (SCS, orange color), very severe cyclonic storm (VSCS, red color)

635 and super cyclonic storm (SuCs, magenta color)) that occurred over North Indian Ocean

636 during 2007 - 2013.

637

638
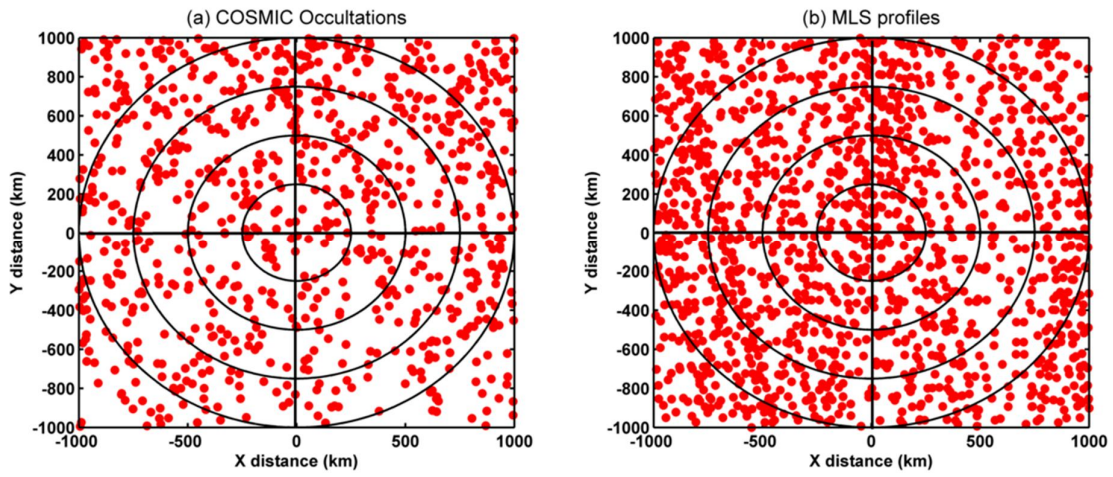
639

Figure 2. Cyclone-centred composite of total available (a) COSMIC GPS RO occultations

and (b) MLS profiles obtained from all the 16 cyclones that are used in the present study.

642
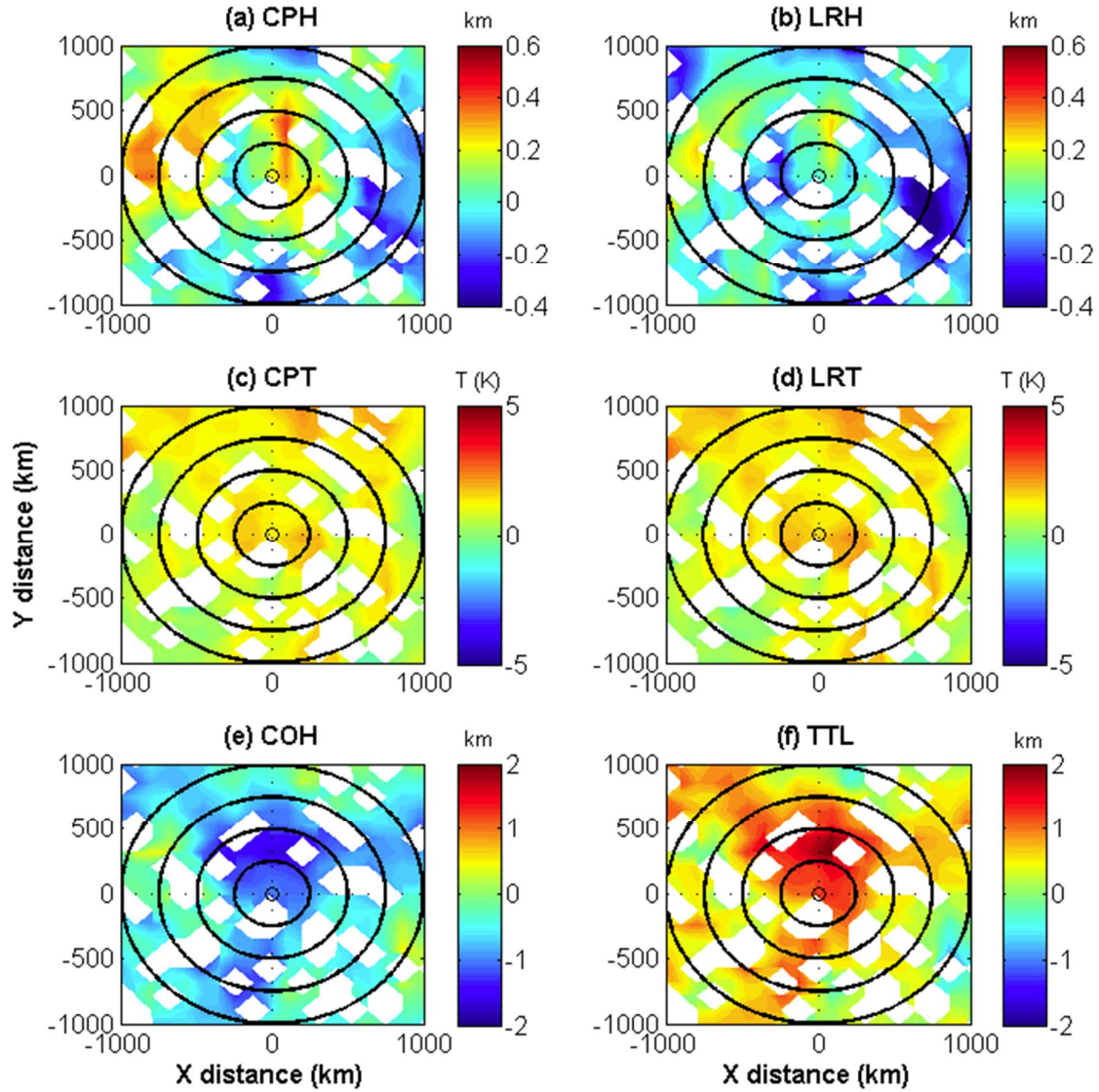
Figure 3. Cyclone centered – composite of mean difference in the tropopause parameters between climatological mean (2002-2013) and individual tropopause parameters observed during cyclones (irrespective of cyclone intensity) in (a) CPH (km), (b) LRH (km), (c) CPT (K), (d) LRT (K), (e) COH (km) and (f) TTL thickness (km). Black circles are drawn to show the 250 km, 500 km, 750 km and 1000 km away from cyclone center (taken from Ravindra Babu et al., ACP, 2015).

651

Figure 4. Normalized cyclone centered – composite of mean ozone mixing ratio observed during cyclones (irrespective of cyclone intensity) at (a) 82hPa, (b) 100hPa, (c) 121hPa, (d) 146 hPa levels by MLS during 2007-2013. (e) to (h) same as (a) to (d) but for normalized mean difference in the ozone mixing ratio between climatological mean (2007-2013) and individual events. Black circles are drawn to show the 250 km, 500 km, 750 km and 1000 km away from cyclone center. Sectors showing C1 (NW), C2 (NE), C3 (SW) and C4 (SE) are also shown in (a).

659
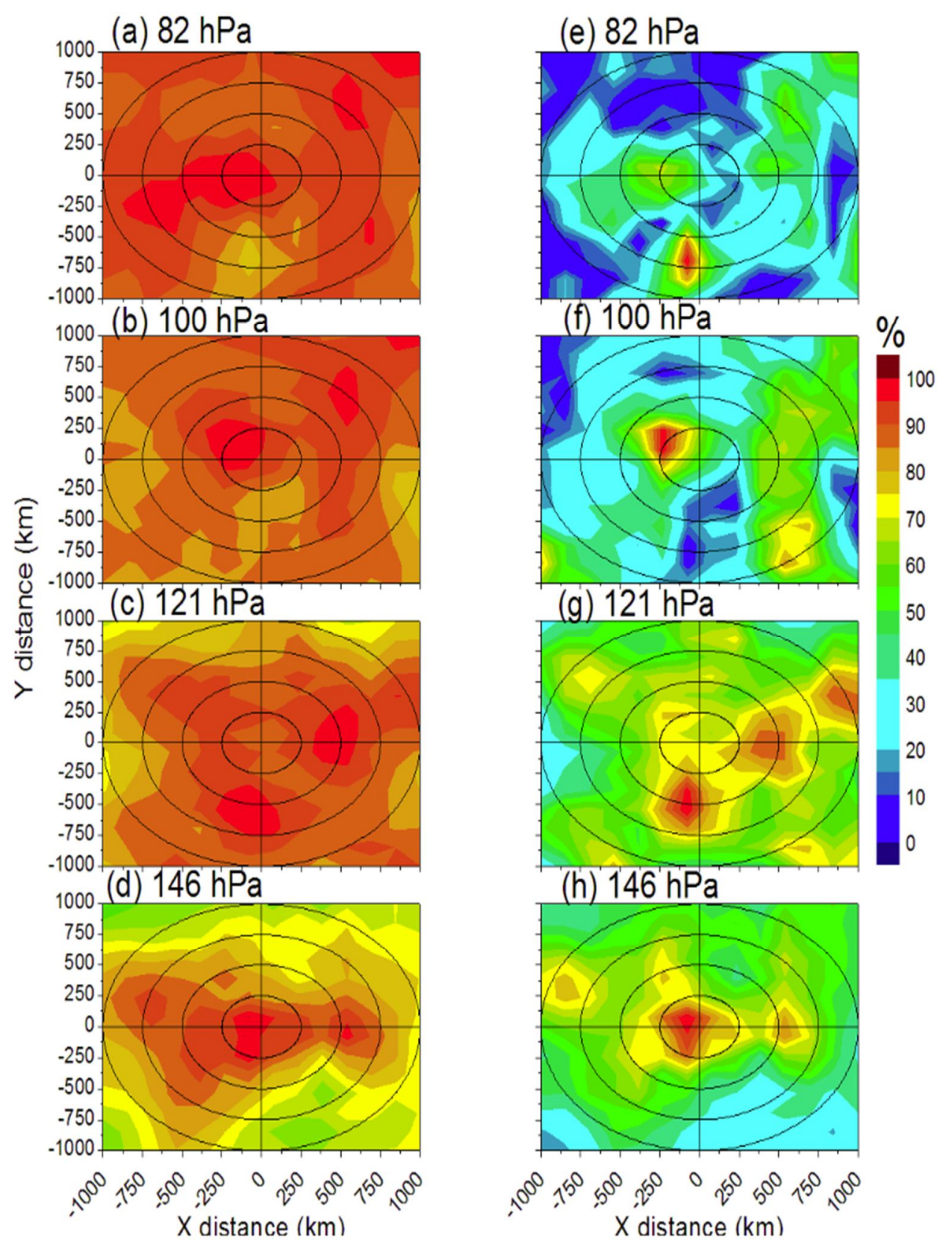
Figure 5. Same as Fig. 4, but for water vapor mixing ratio.

661

662
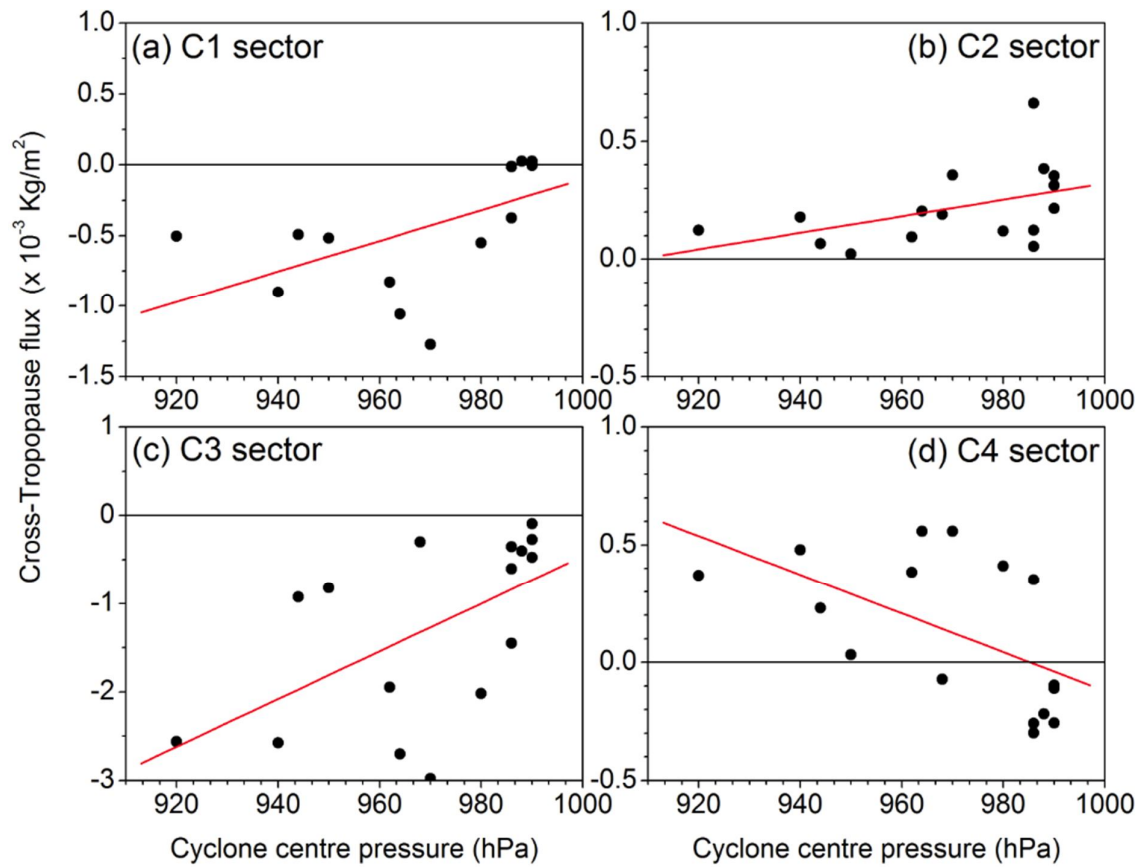
663

664   **Figure 6.** Cross-tropopause flux estimated in the (a) C1 (NW), (b) C2 (NE), (c) C3 (SW), and

665   (d) C4 (SE) sectors from the centre of cyclone for different cyclone intensities (estimated

666   based on cyclone centre pressure). Red lines show the best fit.

667

668

669

670

671
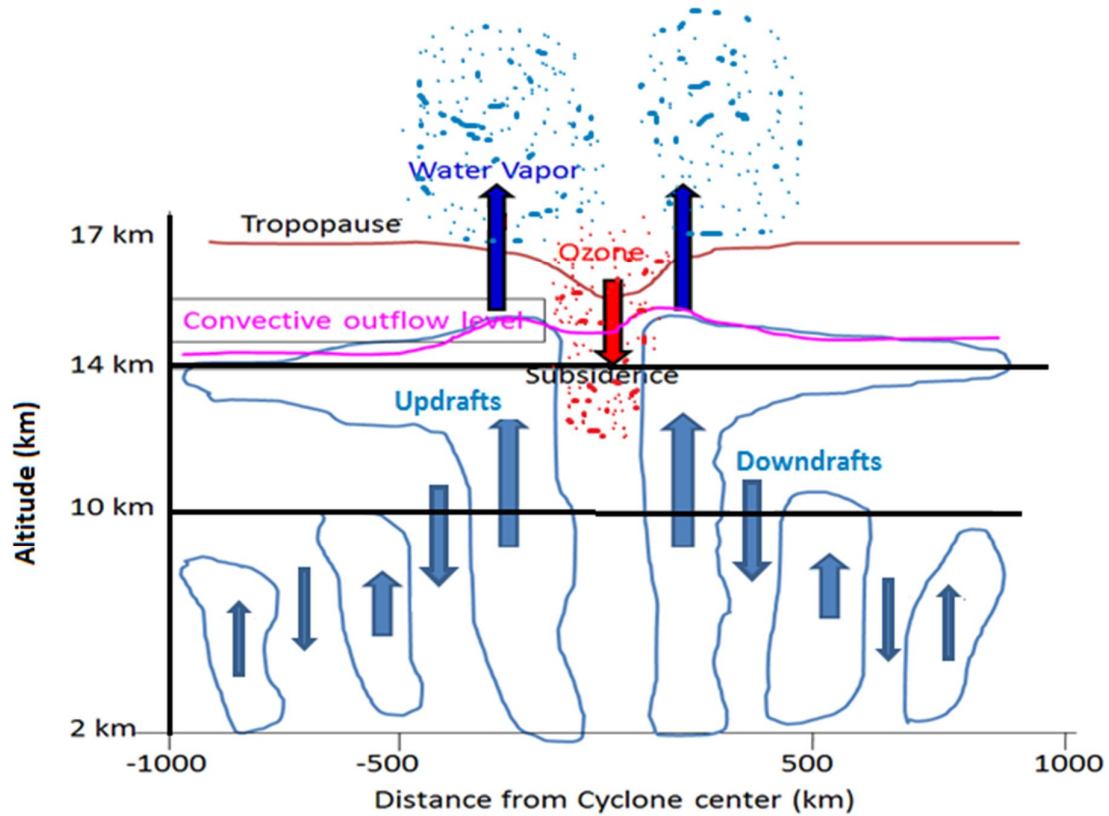
672

Figure 7. Schematic diagram showing the variability of CPH (brown color line) and COH (magenta color line) with respect to the centre of cyclone. Spiral bands of convective towers reaching as high as COH are shown with blue color lines. Light blue (red) color up (down) side arrow shows the up drafts (downdrafts/subsidence). Thickness of the arrows indicates the intensity.